



Behavioral Study of Raft Reinforced with Geogrid and Geocell Through Experiments and Neural Models

Kumar, V.^{1*}, Priyadarshee, A.², Chandra, S.³, Jindal, A.⁴ and Rana, D.⁴

¹ Assistant Professor, Department of Civil Engineering, SoET Block, Central University of Haryana, Mahendergarh, India.

² Assistant Professor, Department of Civil Engineering, MIT Muzaffarpur, Bihar, India.

³ Ph.D. Candidate, Scientist, CSIR-NEERI, Delhi Zonal Centre, India.

⁴ Assistant Professor, Department of Civil Engineering, School of Engineering and Technology, Central University of Haryana, India.

© University of Tehran 2022

Received: 02 Jun. 2022;

Revised: 29 No. 2022;

Accepted: 16 Jan. 2023

ABSTRACT: The stability of a structure could be achieved either by adopting strong foundation or by improving the strength of the soil. This study is an attempt to investigate the behavior of a raft foundation ($U-R_F$) upon reinforcing with geogrid (R_F-R-G_r) and reinforcing with geocell (R_F-R-G_c). The results of the study showed that optimal depth for placement of geogrid was found to be $0.3B$ (B is width of raft) while optimal depth for geocell varied from $0.1B$ to $0.15B$. It was also found that the Bearing Capacity Ratio (BCR) for R_F-R-G_r was typically six times higher than $U-R_F$, while for R_F-R-G_c it was eleven times higher than $U-R_F$. Further, the outcomes of experimental study were modeled using Artificial Neural Networks (ANN) to predict the settlements. It was found that ANN models predicted settlement with higher values of correlation coefficient (r) as 0.9996 for R_F-R-G_r and 0.9995 for R_F-R-G_c .

Keywords: ANN, BCR, Geocell, Geogrid, Raft.

1. Introduction

India is accelerating at a rapid rate on the infrastructural front with smart city based development implemented in different parts of the country. These developments in the geographically diverse country are challenged with existing topography and varied soil conditions. The challenges range from stability of substructure to durability of the superstructure. The focus on substructure is obvious of the fact that big and complex structures like skyscrapers, bridges, and industrial plants, etc. require

stable and economical foundations.

A raft foundation (UR_F) is generally used when the area required under the isolated footing is much higher for the distribution of load with low bearing capacity of soil. However, under poor soil conditions the raft undergoes differential settlement in instances. In such cases, available ground improvement techniques like utilization of the admixture, stone column, soil reinforcement, etc., can be implemented (Jindal and G.D. Ransinchung, 2021, Priyadarshee et al., 2020; Verma et al., 2018; Kumar and Thyagaraj, 2020). Also,

* Corresponding author E-mail: vikaskumarnitk@gmail.com

to improve the behavior of the raft different geosynthetic materials are brought into applications with soil strata. The inclusions of geogrid and geocell as reinforcement has opened new avenues for the constructions of structures even in those areas too which have poorly graded sand beds. In this study, the behavior of raft reinforced with geogrid (R_F-R-G_r) and raft reinforced with geocell (R_F-R-G_c) were explored under loose sand and dense sand condition.

Reinforced Soil Foundation (RSF) has been an area of interest for various researchers in the past too. Binquet and Lee (1975) evaluated the bearing capacity of sand reinforced with metal strips and later many studies were conducted to evaluate footings rested on reinforced sandy soil. Priyadarshie et al. (2014) discussed that, different forms of reinforcement like planar, geocell etc., are available for improving the BCR of soil; however planar and geocells are the most popular alternatives practiced amongst engineers. In planar reinforcement technique geogrids, geotextiles etc., are placed in layers of soil which mobilizes the reinforcing action through interaction between soil and reinforcement. Different works carried out by researchers such as Adams and collin (1997), Sawaaf (2007), etc., describes the mechanism of planar reinforcement and the factors affecting the same.

Geocell is another important form of reinforcement wherein three-dimensional confinement provided by geosynthetic material resists the deformation during the shearing action which increases the load carrying capacity of soil. Different model tests on shallow foundations like strip footing, circular footing etc., and numerical analysis were carried out by different researchers such as Bathurst and Karpurapu (1993), Latha et al. (2008) and many more.

Most of the studies on model foundation supported by reinforced soil have been done on the isolated foundations. Under the isolated foundations like circular footing, square footing etc., reinforcements are extended beyond the footing. Because of

this additional resistance mobilizes due to additional length of the reinforcement. Also, numerical analysis done by different researchers like Han et al. (2008), Latha et al. (2008) etc. on the foundation supported by reinforced soil, is mainly based on the mesh analysis to predict the performance of soil-foundation system (Han et al. 2008). Also statistical analysis is used for prediction by different researchers. Different studies using ANN have been done on problems like prediction of compressive strength for stabilized soil using ANN, evaluation of lateral spreading using ANN (Baziar et al., 2005), assessing geotechnical properties using neural model models (Yang et al., 2002). A hybrid PSO-ANN model for rock-socketed piles was developed by Armaghani et al. (2017) for predicting the ultimate bearing capacity. The intricate problems in geotechnical engineering have used AI models for comparatively better results than statistical models as discussed by Suman et al. (2016) and Doley et al. (2021, 2022).

However, performance of the planar reinforcement and geocell reinforcement is not yet properly investigated under the raft foundation. This study, thus investigates the performance of soil reinforced with planar and geocell reinforcement under raft footing. Also, a comparative study is done to understand the relative performance of these reinforcement under the raft footing. Under different experimental setups, series of test are performed on the reinforced soil-raft foundation systems. Also, to predict the load carrying capacity of the reinforced soil Artificial Neural Network (ANN) is applied in the present study.

2. Methodology and Test Set up

The methodology adopted for this study is illustrated in Figure 1. For studying the performance of $U-R_F$, R_F-R-G_r and R_F-R-G_c , model raft $300\text{ mm} \times 300\text{ mm} \times 25\text{ mm}$ was prepared, and property of sand were investigated. The photographic view of raft and testing tank are shown in Figures 2a and

2b.

As per the Unified Soil Classification System (USCS), (ASTM D 2487-06) sand used in this study could be classified as poorly graded sand (SP) as shown in Figure 3. Biaxial geogrid made of polypropylene was used in this study as planar reinforcement and for preparation of geocell. The Height of Geocell (HG) used in R_F-R-G_c was equal to the number of geogrid layers used for preparation of geocell. The photographic view of geogrid and geocell are shown in Figures 4a and 4b.

The resultant load-deformation behavior of geogrid is presented in Figure 5 as per ASTM D 6637-01. Experimental test series was designed to conduct tests on UR_F , R_F-R-G_r and R_F-R-G_c . The test series G_0 were conducted on unreinforced raft at 40% and 70% Relative Density (RD). In case of R_F-R-G_r and R_F-R-G_c , the laboratory tests were conducted under test series G_1, G_2, G_3, G_4 and G_{C1}, G_{C3}, G_{C5} , respectively, as shown in Table 1. The schematic diagram for R_F-R-

G_r and R_F-R-G_c is shown in Figures 6a and 6b. For R_F-R-G_r , the design variables were $N, b/B, d_r, u/B$ and for R_F-R-G_c , the variables were $h_g/$ and U_g .

2.1. Development of Neural Models

Artificial Neural Network (ANN) models using feed-forwarded and back propagated technique were used for making the neural model for this study. The basic structure of the neural network is divided into three components namely input layer, hidden neuron and output. For optimization of the ANN, fixation of neurons was done by trial-and-error method. The architecture of neural model for geogrid and geocell is shown in Figures 7a and 7b, respectively. The database consisted of matrix of outcomes of experiments for R_F-R-G_r and R_F-R-G_c for constructing neural model. For training the neural model, 70% data was used and 30% data was used for testing the model.

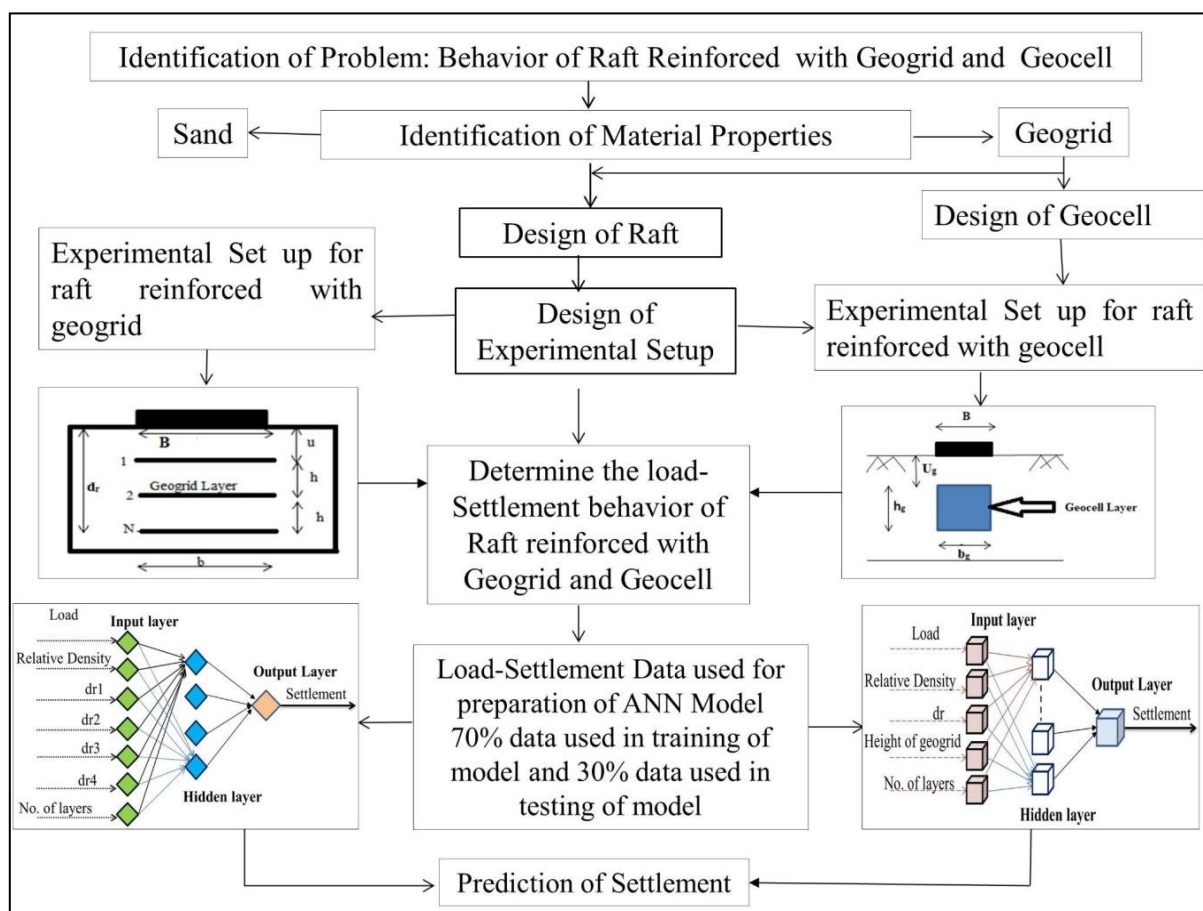
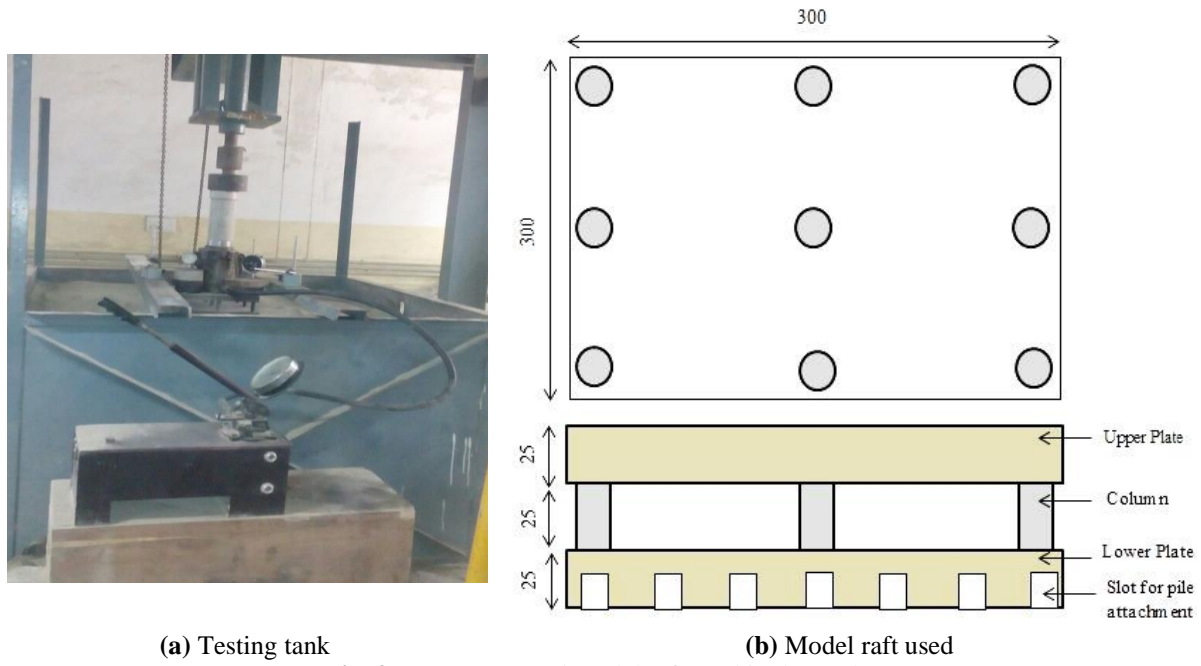


Fig. 1. Methodology employed in study



(a) Testing tank (b) Model raft used
Fig. 2. Test Set up and model raft used in the study

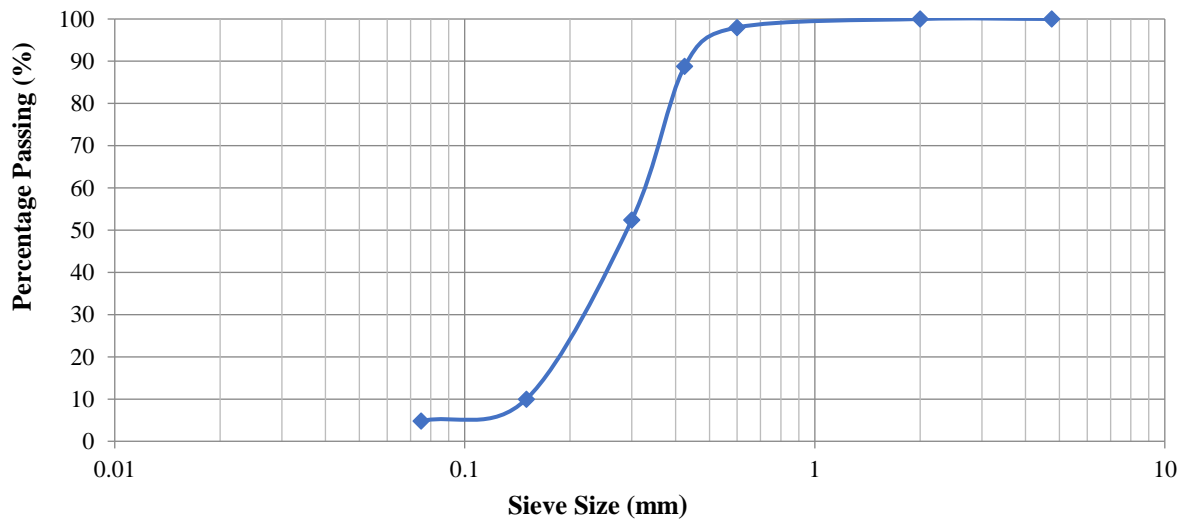


Fig. 3. Grain size distribution of sand

Table 1. Test details for U-R_F, R_F-R-Gr and R_F-R-G_c

| RD (%) | Test series | U-R _F and R _F -R-G _r | | | R _F -R-G _c | |
|-----------------------|----------------|---|-------------------|------|----------------------------------|-------------------|
| | | Number of layer (N) | d _r /B | U/B | Test series | U _g /B |
| 40,70 | G ₀ | ---- | ---- | ---- | ---- | --- |
| | G ₁ | 1 | 0.1 | 0.1 | G _{C1} | 0.1 |
| | | | 0.3 | 0.3 | | 0.3 |
| | | | 0.5 | 0.5 | | 0.5 |
| | | | 0.7 | 0.7 | | 0.7 |
| | G ₂ | 2 | 0.1 and 0.3 | 0.1 | G _{C3} | 0.1 |
| | | | 0.1 and 0.5 | 0.1 | | 0.3 |
| | | | 0.1 and 0.7 | 0.1 | | 0.5 |
| | | | 0.3 and 0.5 | 0.3 | | 0.7 |
| | G ₃ | 3 | 0.3 and 0.7 | 0.3 | G _{C5} | 0.1 |
| | | | 0.3 and 0.7 | 0.3 | | 0.3 |
| | | | 0.5 and 0.7 | 0.5 | | 0.5 |
| | | | 0.1, 0.3 and 0.5 | 0.1 | | 0.7 |
| | G ₄ | 4 | 0.3, 0.5 and 0.7 | 0.3 | G _{C5} | 0.3 |
| 0.1, 0.3, 0.5 and 0.7 | | | 0.1 | 0.5 | | |
| | | | | | 0.7 | |

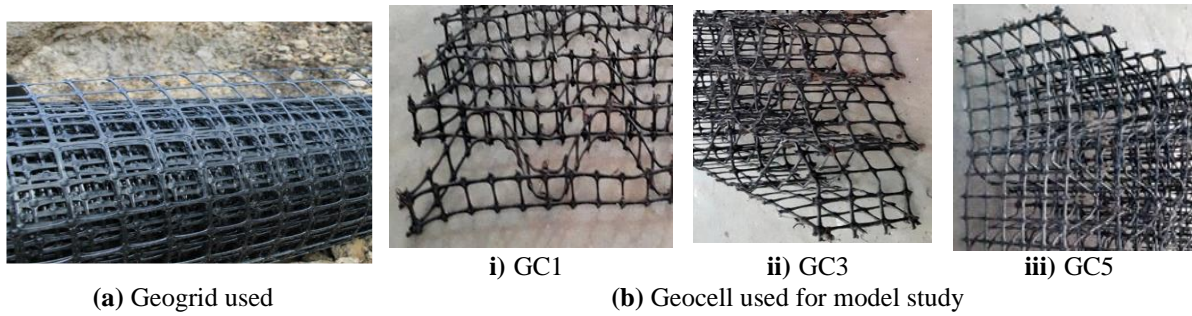


Fig. 4. Geogrid and Geocell used in the study

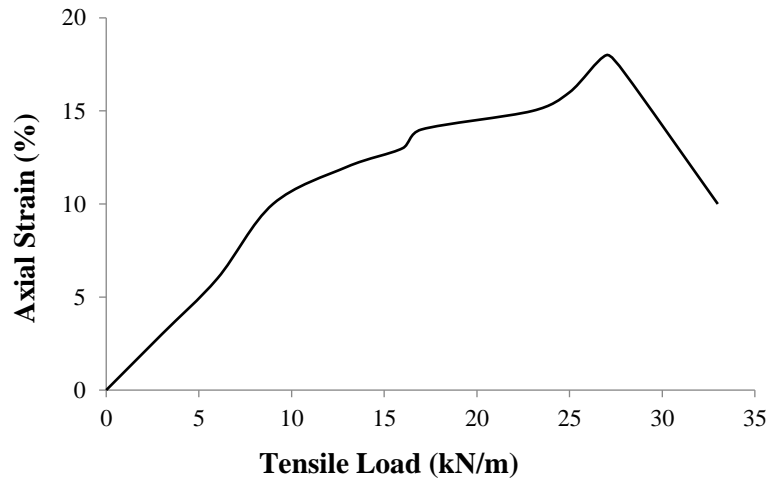


Fig. 5. Load-deformation behavior of biaxial geogrid used in the study

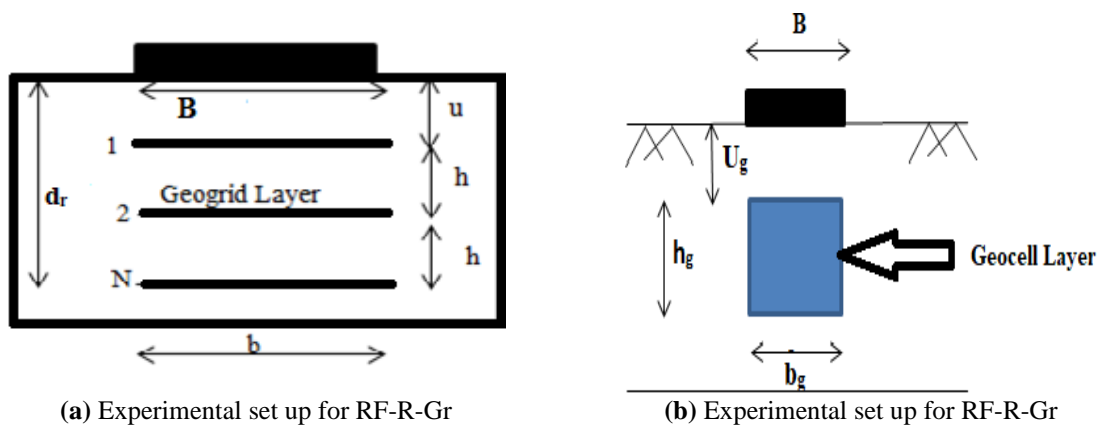


Fig. 6. Experimental Setup for Reinforced foundation

3. Results and Discussion

The effect of design variables considered for U-R_F, R_F-R-G_r and R_F-R-G_c model tests are discussed in the following section. The results obtained were further used to develop a prediction neural model. For comparing the performance of reinforcements, parameters like density, type of reinforcement, reinforcement's top-spacing and number of layers are discussed.

3.1. Effect of Density

Direct Shear test was conducted to study the interaction effect of geogrid with sand. From Figure 8, it can be inferred that peak shear stress would increase with increase in the relative density of soil. This enhancement will increase with the inclusion of planar reinforcement. Peak stress was improved from 65.49 kN/m² to 74 kN/m² for unreinforced sand and from 75.54 kN/m² to 93.05 kN/m² for reinforced sand when the relative density was observed to be increased from 40% to 70%.

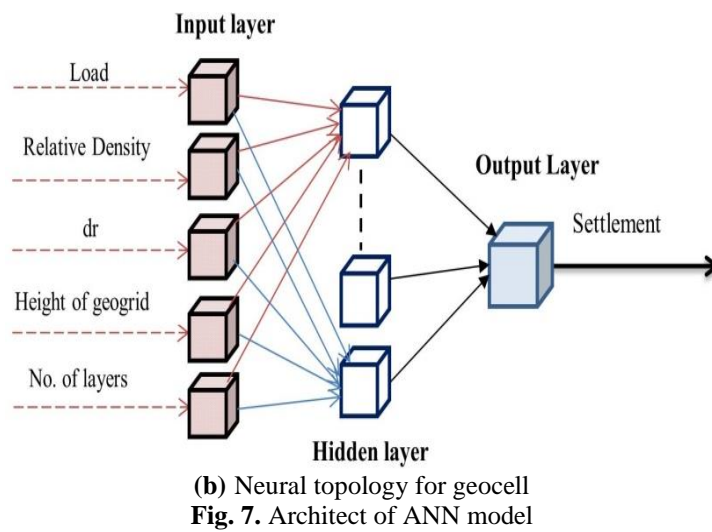
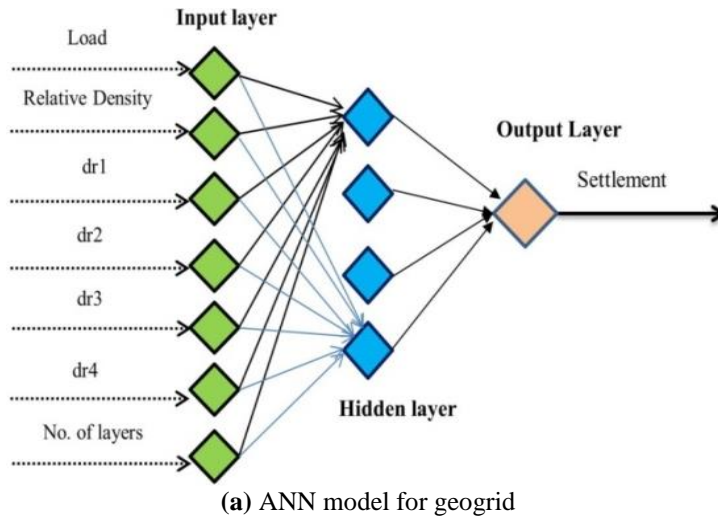


Fig. 7. Architect of ANN model

For R_F - R_G : dr1, dr2, dr3 and dr4 represent different depths of reinforcement when one, two, three and four layers were used, respectively.

No. of layers = No. of geogrid layers.

For R_F - R_G : dr = different depth of reinforcement (30 mm, 90 mm, 150 mm).

Height of geocell = No. of layers \times 30 mm

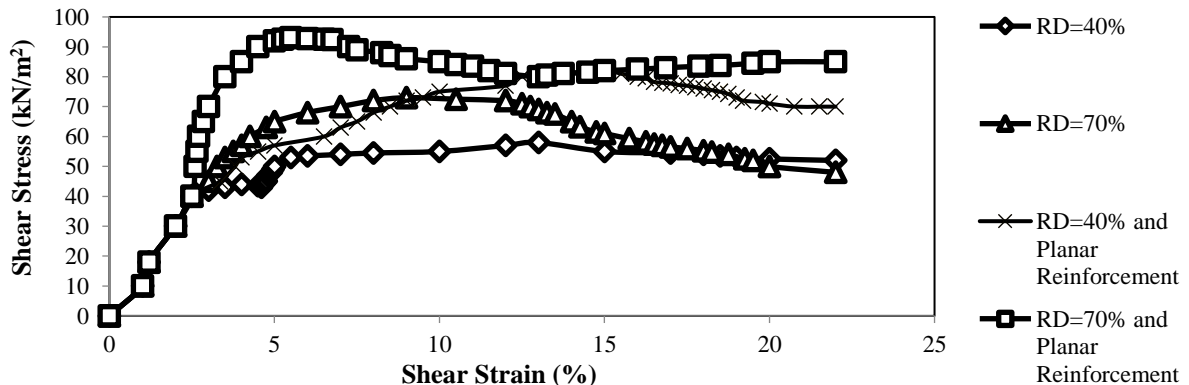


Fig. 8. Stress-strain response for reinforced and unreinforced sand at different relative densities

3.2. Effect of Reinforcement

The pressure–settlement responses were compared through a non-dimensional parameter i.e. Bearing Capacity Ratio

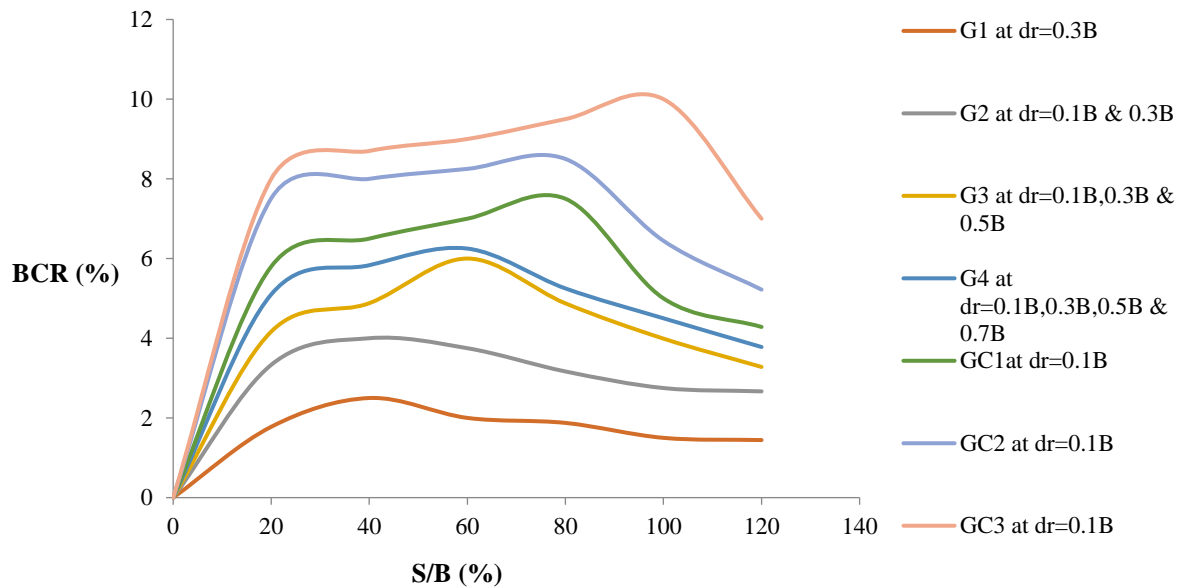
(BCR) as in Eq. (1).

$$BCR = \frac{q_{UR}}{q_U} \tag{1}$$

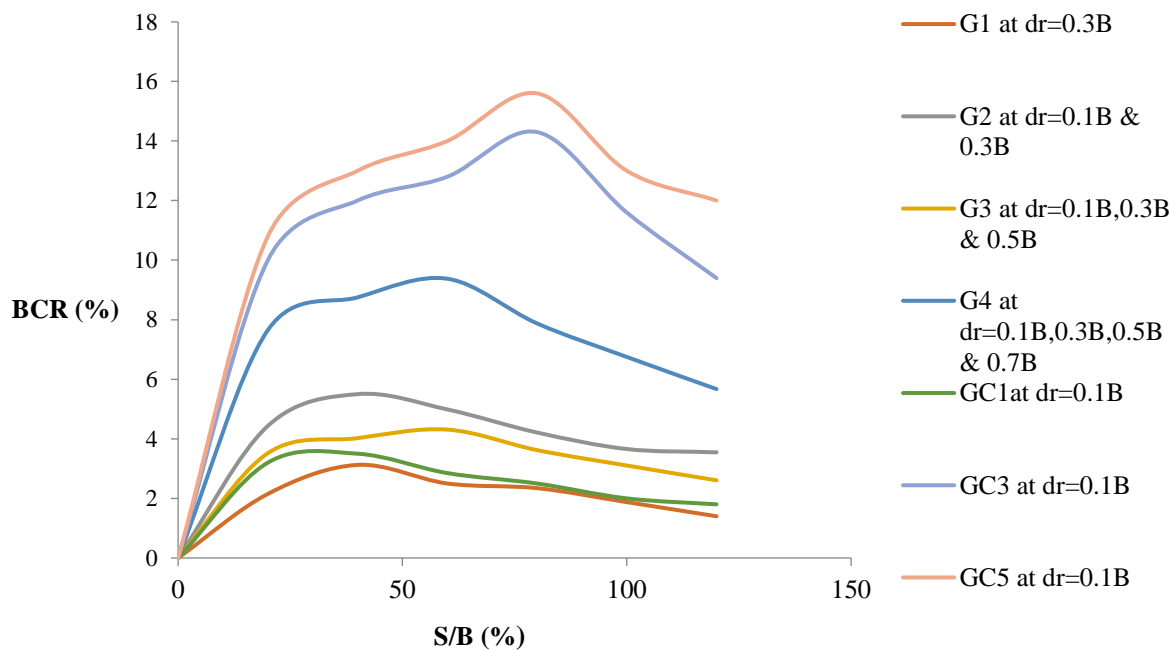
where, q_{UR} : is bearing capacity of reinforced foundation and q_U : is bearing capacity of U- R_F .

The BCR for R_F - R - G_r was typically five times higher than that of U- R_F while for R_F - R - G_c it was seven times than that of U- R_F as shown in Figures 9a and 9b. This is due to

the fact that geocell confine the sand more significantly as compared to geogrid. Also an anchorage action will take place if foundation is reinforced by geocell which develop the hoop stress. This combined action resulted in significant improvement in the BCR.



(a) Pattern of BCR for RF-R-Gr and RF-R-Gc at RD = 40%



(b) Pattern of BCR for RF-R-Gr and RF-R-Gc at RD = 70%

Fig. 9. Effect of relative density on reinforced foundation

3.3. Effect of Reinforcement's Top Spacing for Geogrid and Geocell reinforced foundation

In case of R_F - R - G_r , the distance of first

layer of reinforcement from the base of footing shall mobilize the tensile forces developed which are directly proportional to the depth of the reinforcement. As the

depth of reinforcement below the raft increases, these tensile forces decrease. From Figure 10a it could be inferred that for R_F-R-G_r the optimal results were achieved at $u/B = 0.3$ and the maximum improvement in BCR was obtained at $S/B = 20\%$.

From test results, it is observed that R_F-R-G_c provides better performance than $U-R_F$ and R_F-R-G_r in all cases. This improvement in performance is owing to interface friction developed between soil and 3-dimensional geocell which developed the confinement effect. From Figures 10b it is inferred that for R_F-R-G_{c1} the optimal results were achieved at $U_g/B = 0.15$ and the maximum improvement in BCR was obtained at $S/B = 30\%$

3.4. Effect of Number of Layers

For R_F-R-G_r the maximum significant improvement in BCR was achieved when three layers were used as in test series G_3 . Therefore, it can be concluded that further addition of number of geogrid layers does not affect the bearing capacity of soil significantly, while in case of R_F-R-G_c best results were obtained at test series $GC3$ as

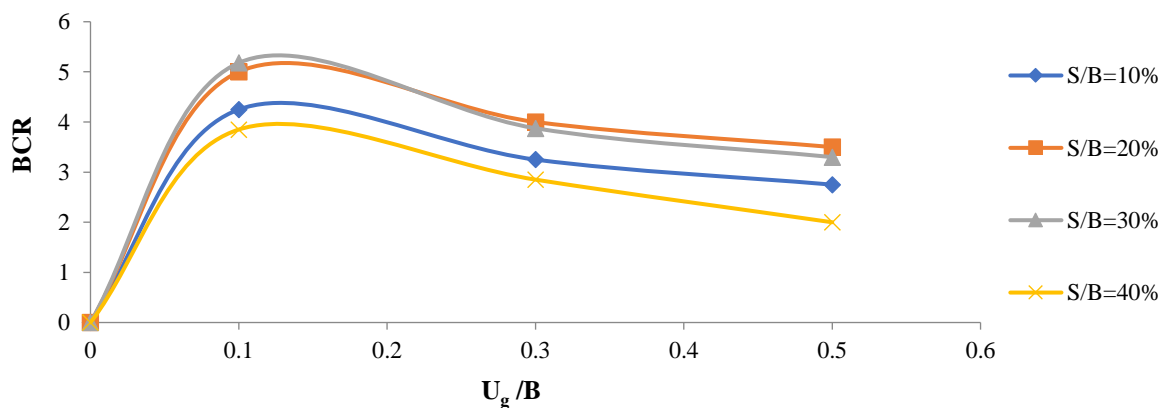
shown in Figure 11.

3.5. Neural Models

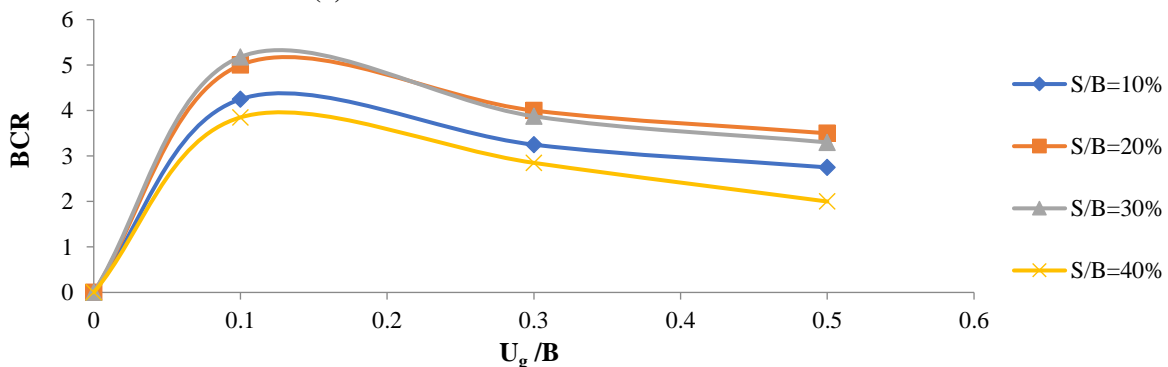
The final topology for any neural model is obtained after finalizing the parameters like activation function, neurons in middle hidden layer, stopping criteria etc. The connections between the layers were logsigmoid and purelin. The first connection was logsigmoid and purelin was a successive function. Least Root Mean Square Error (RMSE) during testing was used for neurons selection in middle layer. Therefore, for R_F-R-G_r the topology was 7-12-1 and for R_F-R-G_c it was 5-11-1 as shown in Figure 12.

3.5.1. Performance of Neural Model

For identifying the performance of ANN, different performance variables (Kumar and Kumar, 2018) as shown in Table 2 were calculated. The performance variables help in deciding the goodness of developed neural models. The predicted results from the model are shown in Figure 13.



(a) BCR versus u/B for test series G1 at RD = 40%



b) BCR versus U_g/B at RD = 70% for test series GC1

Fig. 10. Effect of reinforcement top spacing on reinforced foundation

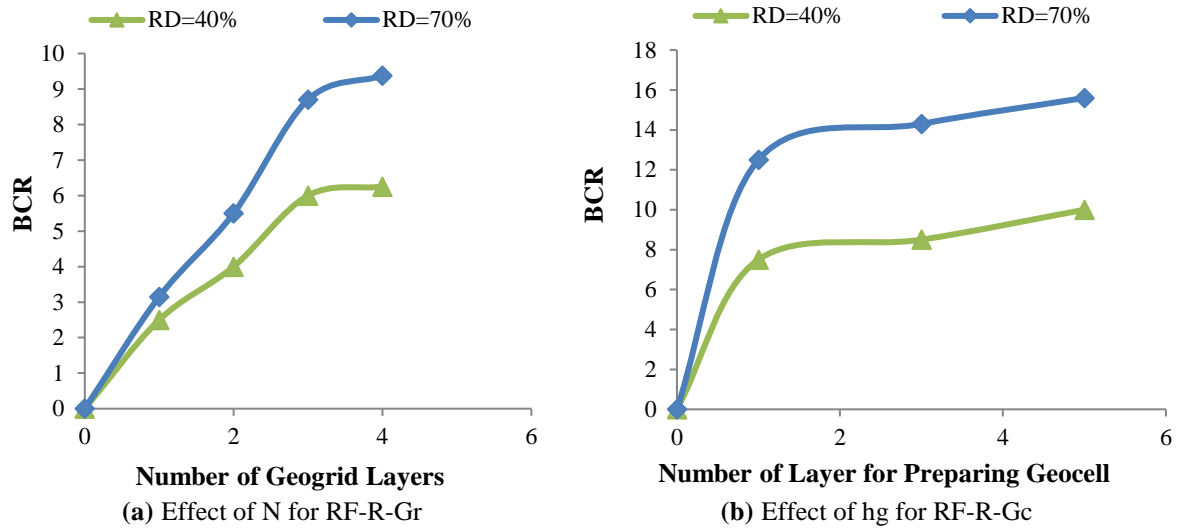


Fig. 11. Effect of reinforcement layer

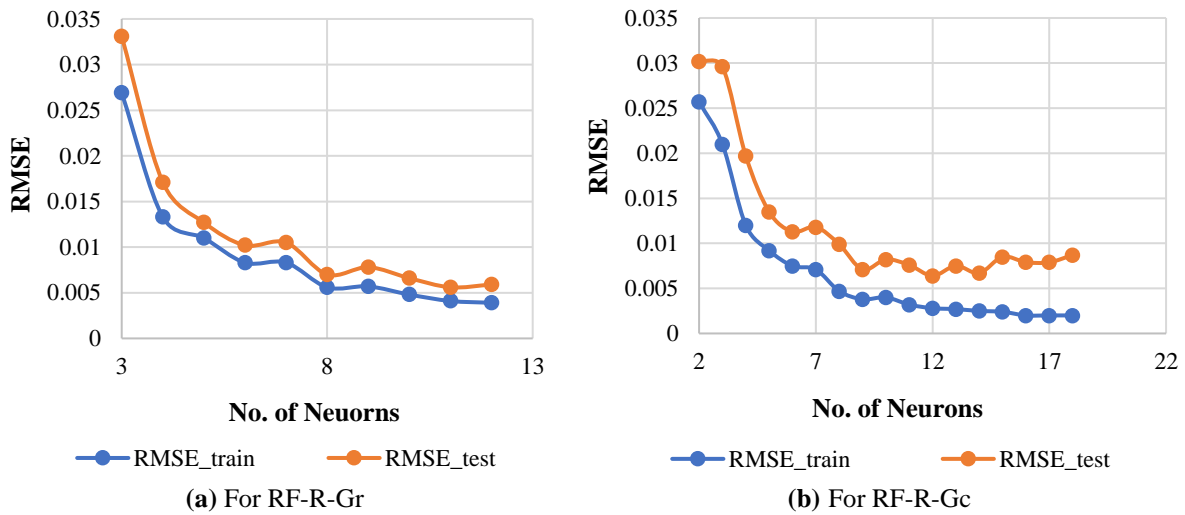
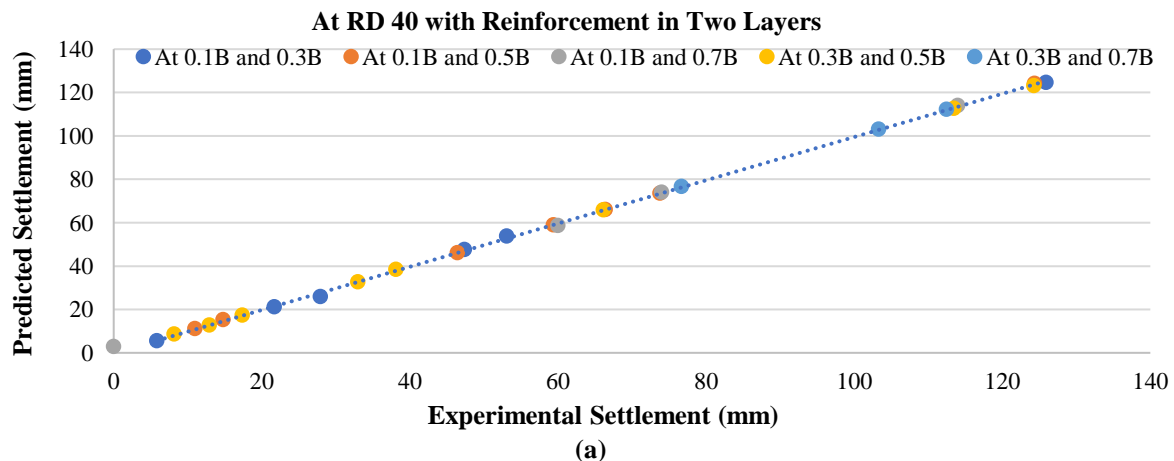


Fig. 12. Pattern of RMSE during training and testing

Table 2. Assessment of performance variables for Geogrid and Geocell

| | MAE | RMSE | CF | r |
|----------------|-------|-------|-------|--------|
| Geogrid | | | | |
| Training | 0.002 | 0.003 | 0.999 | 0.9998 |
| Testing | 0.004 | 0.006 | 0.999 | 0.9996 |
| Geocell | | | | |
| Training | 0.003 | 0.004 | 0.999 | 0.9997 |
| Testing | 0.004 | 0.005 | 0.999 | 0.9995 |



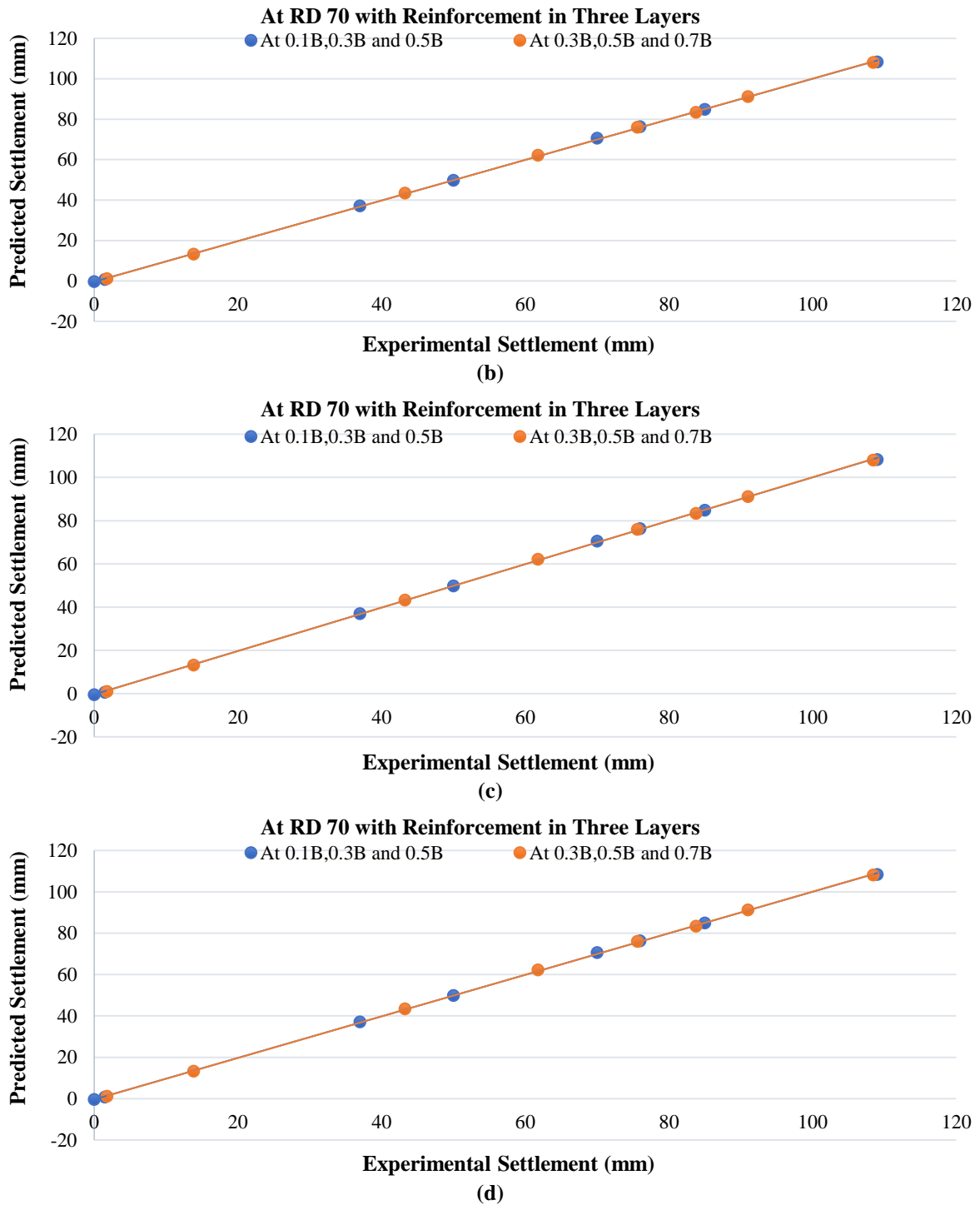


Fig. 12. Pattern of RMSE during training and testing

For R_F-R-G_r , the optimal architecture was obtained as 7-12-1 to predict settlement (S). The weights and biases obtained from trained model for geogrid are shown in Table 3. The Eq. (2) gives output (settlement) by using all input parameters (i.e. Loads (L), Relative Density (RD), dr1, dr2, dr3, dr4 and No. of layers (Nlp)).

For raft reinforced with geocell the optimal architecture obtained was 5-11-1 to

predict settlement (S). The weights and biases obtained from trained model for geocell had been shown in Table 4.

The normalized value of settlement (S) can be calculated using following equation.

$$Settlement = f_{sig}\{b_o + \sum_{k=1}^h [w_k f_{sig}(b_{hk} + \sum_{i=1}^m w_{ik} X(input)_i)]\} \tag{2}$$

Table 3. Connection weights and biases for calculating settlement (Ygc) i.e. for raft reinforced with Geogrid

| Hidden neuron | Weights | | | | | | | Bias | | |
|---------------|----------|-----------------------|----------|---------|---------|---------|----------------------------|----------------|--------------|--------------|
| | w_{ik} | | | | | | | w_k | b_{hk} | b_o |
| | Inputs | | | | | | | Output | Hidden layer | Output layer |
| (k = 1 to 12) | Load (L) | Relative density (RD) | dr1 | dr2 | dr3 | dr4 | No. of layers (N_{lp}) | Settlement (S) | | |
| 1 | 2.8042 | 3.4678 | 2.1315 | 3.0136 | 3.8188 | -0.2099 | -3.0085 | 0.5280 | -0.6778 | 0.0120 |
| 2 | -8.4476 | -4.2540 | -4.0283 | 0.6813 | -0.1670 | -1.3368 | 7.3752 | -0.0794 | 3.9817 | |
| 3 | -2.4716 | -8.1776 | -14.7238 | -0.0437 | 4.5439 | 0.7352 | -11.6633 | 0.5249 | -5.3355 | |
| 4 | 2.1153 | -0.3233 | 0.3523 | -2.9803 | -3.7383 | 0.4669 | 3.2740 | 1.1401 | -4.4261 | |
| 5 | -1.7771 | 0.7992 | -6.0401 | -0.8943 | -0.3476 | 0.6638 | 4.6114 | 1.2843 | -3.0169 | |
| 6 | 2.1295 | -0.2827 | 0.2917 | 0.2573 | 0.0546 | 0.6708 | -1.7831 | 2.8495 | 2.2199 | |
| 7 | 1.9098 | -0.3136 | -0.0572 | 0.7825 | 0.1691 | 0.5006 | -1.5603 | 4.6961 | -0.9630 | |
| 8 | 1.2493 | -0.5264 | -1.3923 | 0.4040 | -2.2094 | 4.4762 | 5.6170 | -2.8879 | 2.4666 | |
| 9 | -0.9754 | 0.1731 | 2.8333 | 0.4662 | 2.2984 | -4.3208 | 4.5377 | 2.8611 | 0.8589 | |
| 10 | 0.7209 | -0.5175 | -2.4152 | -0.7004 | -1.3631 | -4.1193 | 2.7417 | -4.4829 | -0.5241 | |
| 11 | 0.5201 | 0.7982 | 2.9534 | 0.5987 | 2.1740 | 0.5332 | -1.4558 | -1.8853 | 0.6765 | |
| 12 | 0.4852 | -1.6963 | 3.8710 | -7.8275 | -0.2785 | 1.3689 | 7.4323 | -1.3636 | -3.5628 | |

where f_{sig} : represent the transfer function (here is log-sigmoid), b_o : is bias at output layer, w_k : is weight connection between 'k' of the hidden layer and the single output neuron, b_{hk} is bias at neuron 'k' of the hidden layer (k = 1, h), w_{ik} : is weight connection between input variable i and neuron k of the hidden layer and $X(input)_i$: is the input parameter.

4. Conclusions

Study showed the effectiveness of using planar reinforcement and geocell as settlement reduction measure with the rafts. In general, the extra strength was observed due to geocell-reinforcement which is to be dependent on the number of the geocell layers and thickness of geocell used to reinforce the soil. The BCR for R_F-R-G_r

was typically six times higher than that of U-R_F while for R_F-R-G_c was eleven times than that of U-R_F. It was observed that relative density plays a significant role in improving the bearing capacity of soil. The effect of reinforcement was almost double in case of reinforced raft as compared to U-R_F. The optimal depth for placement of geogrid was obtained as 0.3B and for geocell it was 0.15B. In case of reinforced raft, it was observed that with increase in number of layers of geogrid, load intensity was found to be increased at RD 70% more than that for RD 40% however, this effect was observed to be insignificant after an optimum number of reinforcement layers. The lower values of the order of 10^{-3} for MAE and RMSE shows that the neural models are well trained and tested and can be used for solving complex geotechnical problems.

Table 4. Connection weights and biases for calculating settlement (Ygc) i.e. for raft reinforced with geocell

| Hidden neuron | Weights | | | | | Bias | | |
|---------------|----------|-----------------------|---------|-----------------------------|----------------------------|----------------|--------------|--------------|
| | w_{ik} | | | | | w_k | b_{hk} | b_o |
| | Inputs | | | | | Output | Hidden layer | Output layer |
| (k = 1 to 11) | Load (L) | Relative density (RD) | dr | Height of Geogrid (h_g) | No. of layers (N_{lg}) | Settlement (S) | | |
| 1 | 4.6619 | -0.1100 | 0.3989 | -0.5677 | -1.4156 | 0.7687 | -2.9583 | 2828.9116 |
| 2 | -0.9584 | -0.0199 | 1.4175 | 1.6667 | -0.3249 | -2829.0547 | 10.1704 | |
| 3 | -1.6689 | 2.6778 | -1.6870 | -2.6193 | -1.1327 | -0.6833 | 1.0955 | |
| 4 | 1.0102 | 1.5909 | 0.7418 | 2.0951 | 0.3838 | -153.4224 | 1.3146 | |
| 5 | -1.6498 | 0.2736 | -2.5507 | 1.0150 | -0.5241 | 0.3931 | -1.2418 | |
| 6 | -5.1185 | 9.4275 | -6.9803 | -4.9604 | -4.1751 | 0.1176 | 1.1746 | |
| 7 | -2.6048 | -1.5796 | 2.1554 | -2.3718 | -2.0127 | 0.2284 | 0.3234 | |
| 8 | -1.2315 | 0.3857 | 30.4316 | 15.1914 | 16.4570 | 0.8228 | 37.0194 | |
| 9 | 1.0003 | 1.5870 | 0.7434 | 0.4169 | 2.0675 | 152.8009 | 1.2982 | |
| 10 | -2.0663 | 0.0789 | -0.2321 | -0.4019 | 1.5601 | -2.0521 | -0.2065 | |
| 11 | 2.3428 | 2.1446 | 0.5364 | 1.4305 | -0.0262 | 1.0644 | 2.2043 | |

5. References

- Adams, M.T. and Collin, J.G. (1997). "Large model spread footing load tests on geosynthetic reinforced soil foundation", *Journal of Geotechnical and Geoenvironmental Engineering*, 123(1), 66-72, [http://doi.org/10.1061/\(ASCE\)1090-0241\(1997\)123:1\(66\)](http://doi.org/10.1061/(ASCE)1090-0241(1997)123:1(66)).
- Bathurst, R.J. and Karpurapu, R. (1993). "Large-scale triaxial compression testing of geocell-reinforced granular soils", *Geotechnical Testing Journal*, 16(3), 296-303, <http://doi.org/10.1520/GTJ10050J>.
- Binquet, J. and Lee, K.L. (1975). "Bearing capacity tests on reinforced earth slabs", *Journal of Geotechnical and Geoenvironmental Engineering*, 101(12), 1241-1255.
- Doley, C., Das, U.K. and Shukla, S.K. (2021) "Response of square footing on geocell-reinforced sand bed under static and repeated loads", *International Journal of Geosynthetics and Ground Engineering*, 7(4), 90, <https://doi.org/10.1007/s40891-021-00336>.
- Doley, C., Das, U.K. and Shukla, S.K. (2022) "Development of a multiple regression equation for prediction of bearing capacity of geocell-reinforced sand beds based on experimental study", *Arabian Journal of Geosciences*, 15(16), 1408, <https://doi.org/10.1007/s12517-022-10652-y>.
- Jahed Armaghani, D., Shoib, R.S.N.S.B.R., Faizi, K. and Rashid, A.S.A. (2017). "Developing a hybrid PSO-ANN model for estimating the ultimate bearing capacity of rock-socketed piles", *Neural Computing and Applications*, 28, 391-405, <https://doi.org/10.1007/s00521-015-2072-z>.
- Jindal, A. and G.D. Ransinchung, R.N. (2022). "Behavioural study of incorporation of recycled concrete aggregates and mineral admixtures in pavement quality concrete", *Civil Engineering Infrastructures Journal*, 55(2), 351-372, <https://doi.org/10.22059/cej.2022.326564.1766>.
- Kumar, K.S.R. and Thyagaraj, T. (2020). "Comparison of lime treatment techniques for deep stabilization of expansive soils", *International Journal of Geotechnical Engineering*, 15(8), 1021-1039, <https://doi.org/10.1080/19386362.2020.1775359>.
- Latha, G.M., Dash, S.K. and Rajagopal, K. (2008). "Equivalent continuum simulations of geocell reinforced sand beds supporting strip footings", *Geotechnical Geology Journal*, 26, 387-398, <https://doi.org/10.1007/s10706-008-9176-5>.
- Priyadarshie A., Chandra S., Gupta D. and Kumar V. (2020). "Neural models for unconfined compressive strength of kaolin clay mixed with pond ash, rice husk ash and cement", *Journal of Soft Computing in Civil Engineering*, 4(2), 87-108, <https://doi.org/10.22115/SCCE.2020.223774.1189>.
- Suman,S., Khan, S.Z., Das, S.K. and Chand, S.K. (2016). "Slope stability analysis using artificial intelligence techniques". *Natural Hazards*, 84(2),727-748, <https://doi.org/10.1007/s11069-016-2454-2>.
- Verma, S., Kumar V. and Priyadarshie A. (2018). "An experimental test study on ring footing resting on clay bed reinforced by stone column", *Innovative Infrastructure Solutions*, 64(3),1-16, <https://doi.org/10.1007/s41062-018-0169-9>.
- Yang, Y. and Rosenbaum, M.S. (2002). "The artificial neural network as a tool for assessing geotechnical properties", *Geotechnical and Geological Engineering*, 20(2), 149-168.



This article is an open-access article distributed under the terms and conditions of the Creative Commons Attribution (CC-BY) license.